Environmental Science and Pollution Research (2023) 30:40576–40587
https://doi.org/10.1007/s11356-022-24930-5

RESEARCH ARTICLE

Using innovative copper-loaded activated alumina (Cu/AA) as the catalyst for catalytic wet peroxidation (CWPO) of catechol

Vijayalakshmi Gosu[1] · Archana Dhakar[1] · Tian C. Zhang[2] · Rao Y. Surampalli[3] · Verraboina Subbaramaiah[1]

Received: 17 September 2022 / Accepted: 19 December 2022 / Published online: 9 January 2023

Abstract

In this study, copper-loaded activated alumina (Cu/AA) was synthesized and used for the CWPO of catechol (a representative refractory organic pollutant). Various characterization techniques were deployed to characterize the catalysts, e.g., activated alumina (AA), as well as pristine and spent 1% Cu/AA. The innovative 1% Cu/AA catalyst exhibited good thermal stability up to 1173 K with a marginal weight loss of 13%. The Cu species were well dispersed on the activated alumina framework with no significant cluster formation. Typically, the average copper particle size of 5 nm was dispersed on the AA framework. Catechol removal was observed to be 92% with 87% mineralization at optimized conditions (initial catechol concentration = 200 mg/L, catalyst dose of 1% Cu/AA = 2 g/L; temperature = 323 K; pH = 6; and H_2O_2/catechol stoichiometric ratio = 0.5). The mineralization of catechol was analyzed using mass spectroscopy, with the associated mechanism has been elucidated. Results of this study indicated that synthesized catalyst has phenomenal advantages in terms of simple separation and high removal efficiency of catechol, suggesting the feasibility of employing Cu/AA as the effective catalyst for the CWPO of catechol.

Keywords Catechol · Activated alumina · CWPO · Mineralization · Copper · Advanced oxidation

Introduction

Catechol (also named 1,2-dihydroxybenzene or pyrocatechol) has been found in the wastewater released from various industries such as textiles, petrochemicals, rubber, dyes, pharmaceuticals, plastics, cosmetics, paper, and pulp, etc. Furthermore, the effluents from coal gasification contain catechol and resorcinol, and their concentrations range from a few mg/L to 1000 mg/L (Subramanyam and Mishra 2007). Moreover, 5500 mg/L of catechol was identified in low-temperature coal carbonization effluents (Aghapour et al. 2015). Catechol is hazardous upon exposure, harmful if inhaled, irritates the skin and eyes, affects the respiratory tract, destroys DNA, and accumulates in the bone marrow due to its aromatic nature (Kumar et al. 2003). Catechol is considered carcinogenic to humans and is more toxic than phenol and resorcinol (Thakur et al. 2017). Numerous treatment methods have been explored for catechol-bearing wastewater, including adsorption, chemical oxidation, biological process, precipitation, and advanced oxidation processes (AOPs) (Mukherjee et al. 2007). Of these methods, several AOPs have been investigated for the treatment of catechol-containing wastewater, including catalytic ozonation (Moussavi et al. 2014; Aghapour et al. 2015; Kermani et al. 2018), photo-oxidation (Mandal et al. 2004), photocatalysis (M'hemdi et al. 2012), and Fenton (Lofrano et al. 2009; Yang et al. 2016). The advantage of using AOPs compared to the other treatment processes is that AOPs can completely transform the organic components into simple and harmless organic and inorganic species.

Among the different AOPs, the catalytic wet-peroxidation (CWPO) process is considered to be the most cost-effective process for treatment of industrial and urban wastewater (Márquez et al. 2018). CWPO operates at atmospheric pressure and moderate temperature (below 373 K) with either

Responsible Editor: George Z. Kyzas

✉ Verraboina Subbaramaiah
vsr.chem@mnit.ac.in

[1] Department of Chemical Engineering, Malaviya National Institute of Technology, Jaipur 302017, India

[2] Department of Civil & Environmental Engineering, University of Nebraska-Lincoln, Omaha, NE 68182, USA

[3] Environment, and Sustainability (GIEES), Global Institute for Energy, P.O. Box 14354, Lenexa, KS 66285, USA

homogeneous (non-supported) or heterogeneous (supported) catalysts. CWPO with homogeneous catalysts has significant limitations, including pH sensitivity, the likelihood of secondary contamination, high catalyst use, and difficulty with catalyst recycling (Subbaramaiah et al. 2013a; Gosu et al. 2020). Accordingly, CWPO with heterogeneous catalysts (e.g., with the base supporting materials being carbon, clay, organics, and metal) is receiving greater attention. Currently, several heterogeneous catalysts have been investigated, including various active metals (iron, copper, cerium, etc.) supported on silica, granular activated carbon (Gosu et al. 2018c), SBA-15 (Subbaramaiah et al. 2013a, b; Kim et al. 2021), pillared clay (Kıpçak and Kurtaran Ersal 2021; García-Mora et al. 2021), MCM-41 (Hachemaoui et al. 2021), and copper-based catalysts supported on organic material. Some materials used in CWPO are synthesized using Cu^{2+}, Mn^{2+}, and Co^{2+} (Márquez et al. 2018). CWPO of catechol degradation have been investigated using various heterogeneous catalysts such as Fe^{2+}/ H_2O_2 (M'hemdi et al. 2012), Fe supported on clay (Elboughdiri et al. 2015) Fe_3O_4-CeO_2 nanocomposite (Gogoi et al. 2017) and ZVI/Mn-C (Qin et al. 2022). Gogoi et al. (2017) synthesized the Fe_3O_4-CeO_2 metal oxide nanocomposite to evaluate the catalytic activity for the degradation of catechol. Qin et al. (2022) employed the ZVI/Mn-C bimetallic catalyst for the degradation of catechol under neutral conditions using Fenton like process where 100% degradation and 46% COD removal was achieved at optimum conditions.

Among the various supporting materials, alumina has been extensively used as an adsorbent and catalyst support in water and wastewater treatment. It has good adsorptive properties and has been widely deployed to remove various organic contaminants and inorganic contaminants from aqueous solutions (Srivastav and Srivastava 2009). It has also been used as an adsorbent in the adsorptive desulfurization of liquid fuels. Activated alumina (AA) has been used for various industrial applications such as AA supported Cu and Ni employed to synthesize metal-phthalocyanine (Sánchez-De La Torre et al. 2013), Fe/Al_2O_3 catalyst used for catalytic oxidation of phenol (di Luca et al. 2018), mesoporous alumina catalyst utilized for methane-CO_2 reformation (Bian et al. 2021), and nano-porous aluminum employed for hydrogen production. On the other hand, copper oxide catalysts have been reported to be efficient for deep oxidation of carbon monoxide, methane, methanol, ethanol, and acetaldehyde (Cordi et al. 1997). CuO/activated carbon is efficient in degrading organic pollutants (Hu et al. 1999; Gosu et al. 2018b), and copper nitrate is the most effective catalyst for the catalytic oxidation of dye and printing wastewater (Hu et al. 1999).

In light of the aforementioned analysis, AA appears to have potential for the CWPO of catechol because AA is cheaper, easier preparation, and environmentally benign. However, no studies were found in the literature on using AA or AA-supported Cu for the CWPO of catechol. Therefore, we hypothesized that AA-supported catalysts with copper as the active element (Cu/AA) would increase the catalytic activity with high metal dispersion, and thus, can be used to treat catechol-bearing wastewater in the CWPO process. To test these hypotheses, we did this study with the following specific purposes: (a) synthesizing the 1% Cu loaded AA (1% Cu/AA) by the impregnation technique; (b) determining the physico-chemical parameters of 1% Cu/AA by various characterization techniques; (c) optimizing the catalytic performance of 1% Cu/AA for CWPO of catechol in a batch process; and (d) elucidating the catalytic mechanism of catechol degradation/mineralization.

Materials and methods

Materials

Only analytical reagent (AR) grade chemicals were used in this work, and their purity and supplier details are listed in Table 1.

Synthesis of Cu/AA catalysts

The incipient wet impregnation approach was adopted to synthesize the copper-loaded activated alumina (Cu/AA) catalyst (Priyanka et al. 2014). The required amount of

Table 1 Purity and supplier details

Chemical	Purity	CAS number	Source
Catechol	> 98%	120–80-9	Loba Chemie Pvt. Ltd, India
Hydrochloric acid	> 98%	7647–01-0	CDH Pvt. Ltd, India
Activate alumina	> 99%	1344–28-1	ASES chemical works, India
Sodium hydroxide	> 99%	1310–73-2	Fisher Scientific, India
Copper nitrate tri-hydrate	> 98%	10,031–43-3	Merck Specialties Pvt. Ltd, India
H_2O_2 (30 wt%)	> 99%	7722–84-1	Rankem Pvt. Ltd, India
Deionized (DI) water	18 MΩ-cm resistivity		SM laboratories, India

$Cu(NO_3)_2{\cdot}3H_2O$ (0.3825 gm for 1, 0.7650 gm for 2, and 1.9126 gm for 5 wt. % Cu/AA) was dissolved in deionized water. Thereafter, 9.9 gm, 9.8, and 9.5 gm of AA balls were added into the copper dissolved solution of 1%, 2%, and 5 wt.%, respectively with continuous stirring at 500 revolutions per minute (RPM) for 30 min using a magnetic stirrer. The resulting mixture was dried in a vacuum oven for 12 h at 353 K. The dried samples were calcined in a muffle furnace for 4 h at 623 K. The final calcined samples were labeled as 1% Cu/AA, 2% Cu/AA, and 5% Cu/AA.

Catalyst characterization and analytical methods

A UV/VIS spectrophotometer (UV 1800, Shimadzu, Japan) was used to determine the concentration of catechol in the aqueous solution. Catechol concentration before and after treatment was measured by observing absorbance at a wavelength of 275 nm (Aghapour et al. 2015). The TOC (total organic carbon) was measured using a TOC analyzer (Sievers InnovOx TOC Analyzer, SUEZ, USA). A mass spectrometer (Xevo G2-S, Waters, USA) was used to understand the mineralization process in the CWPO process. A 50:50 (v/v) ratio of acetonitrile and water was used as a mobile phase with a flow rate of 1 ml/min. The physicochemical characteristics of the potential catalyst (1% Cu/AA), support (AA), and spent catalyst (1% Cu/AA) were carried out to acquire a better understanding of the synthesized catalysts. The samples' surface functional group and surface chemistry were evaluated using a Fourier transform infrared spectrophotometer (FTIR) (Spectrum Two, Perkin Elmer, USA) with the KBR pellet technique. The surface morphology of samples was evaluated using a scanning electron microscope (SEM) (Nova Nano FE-SEM 450, Thermo Fisher Scientific, USA). Thermal stability of samples was determined using Thermo gravimetric analysis (TGA) (STA 6000, Perkin Elmer, USA) at a heating rate of 10 °C/min over the temperature range of 303–1173 K. The samples' morphology and elemental composition were investigated using a high-resolution transmission electron microscope HR-TEM (Tecnai G2 20 S-Twin, FEI, Netherlands). Energy-dispersive X-ray spectroscopy has been used to evaluate metal dispersion on the support (EDS).

Catalytic wet peroxide oxidation of catechol

The CWPO of catechol was performed in a 250 ml round-bottom flask with three necks. The middle neck contained a reflux condenser, which was used to condense the vapors that were produced throughout the reaction. The other two necks were utilized to collect samples and assess temperature. To maintain a consistent temperature throughout the process, the reactor was placed in an oil bath. The entire reactor system was supported by a magnetic stirrer with a heating element (2MLH, REMI). The reaction's desired temperature was maintained with the aid of a propositional integral controller (PID). The reaction mixture was homogeneously mixed using a magnetic stirrer and set to 300 rpm. A reaction mixture of 100 ml was utilized for each experiment run. The initial pH was adjusted (2–10 pH) using a solution of 0.1 N HCl or 0.1 N NaOH. Once the desired temperature achieved, required amount of catalyst (1% Cu/AA) and oxidizing agent H_2O_2 were added to initiate the reaction. The amount of H_2O_2 was predetermined based on stoichiometry and the assumption that catechol degrades completely, as shown in Eq. (1).

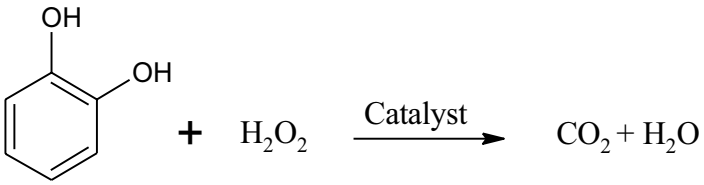

(1)

After 4-h reaction, liquid samples were withdrawn from the flask, and then filtered using a syringe membrane filter (0.45 µm, PTFE2545, MOXCARE). The filtrates of the samples were analyzed with the UV spectrophotometer. Furthermore, the TOC of the filtrates were examined for the mineralization of catechol at optimum conditions (see below). Equation (2) was used to calculate the percentage removal of catechol/TOC

$$\text{Percentage removal of TOC/catechol} = \left(\frac{C_o - C_t}{C_o}\right) \times 100 \quad (2)$$

where C_o (mg/L) represents the initial concentration of TOC or catechol, while C_t (mg/L) denotes the TOC or catechol concentrations after time t. All experiments were repeated three times, and the average of the results was reported.

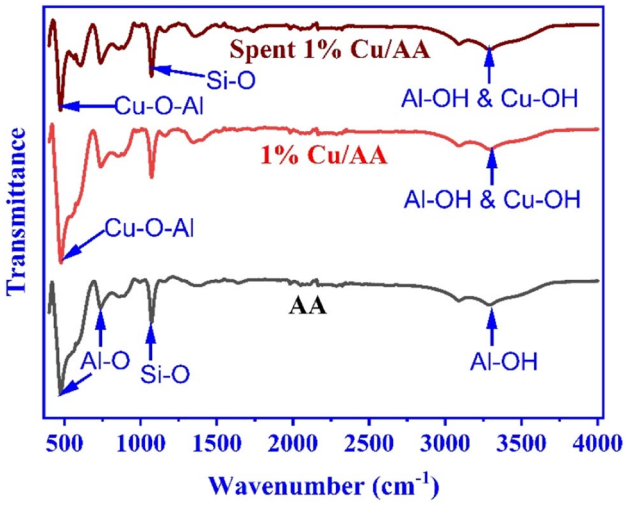

Fig. 1 FTIR spectra of (**a**) spent 1% Cu/AA, (**b**) pristine 1% Cu/AA, and (**c**) AA

Results and discussion

Characterization of synthesized catalyst

The nature of functional groups present on a catalyst may affect its surface behavior. The FTIR spectra of AA, 1% Cu/AA, and spent 1% Cu/AA after CWPO are shown in Fig. 1. The wavelength in the range of 500–1000 cm^{-1} is attributed to Al-O, Cu–O, and Al-O-Cu bending and stretching vibrations in AA, 1% Cu/AA, and spent 1% Cu/AA (Ahmed and Siddiqui 2014). All sample spectra exhibit weak vibration modes in the range 1350–1550 cm^{-1} due to residual organic compounds, which can be assigned to carbonates or carboxylates, as the result of synthesis method used (Zawadzki et al. 2009). The peak at 3200 and 3600 cm^{-1} is attributed to O–H vibration due to physically adsorbed water molecules. FTIR spectra of AA samples show a wide peak 474 and 730 cm^{-1} ascribe the Al-O stretching vibration. The peak at 998 cm^{-1} is attributed to asymmetric stretching of alumino-and silico-oxygen (Mishra et al. 2021). Similarly, the FTIR spectra of 1% Cu/AA showed similar peaks as AA. However, the peak intensity was slightly altered. A similar trend was reported for copper-containing $ZnAl_2O_4$ spinels in the literature (Zawadzki et al. 2009). In the 1% Cu/AA spectra, the peak around 998 cm^{-1} shifted the band, and this may be due to partial dealumination of the framework with copper species. Furthermore, the peak intensity at 476 cm^{-1} was increased in the 1% Cu/AA sample. The FTIR spectra of spent 1% Cu/AA were analyzed, and it was found that there was no significant change in the functional groups. However, medium to weak bands noticed around 620 cm^{-1} could be assigned to vibrational frequencies due to changes in the microstructural features due to the adsorption/desorption of reactant molecules on the catalyst surface (Fasanya et al. 2019).

Figure 2 illustrates the morphology of AA, 1% Cu/AA, and spent 1% Cu/AA. When 1% Cu/AA was compared

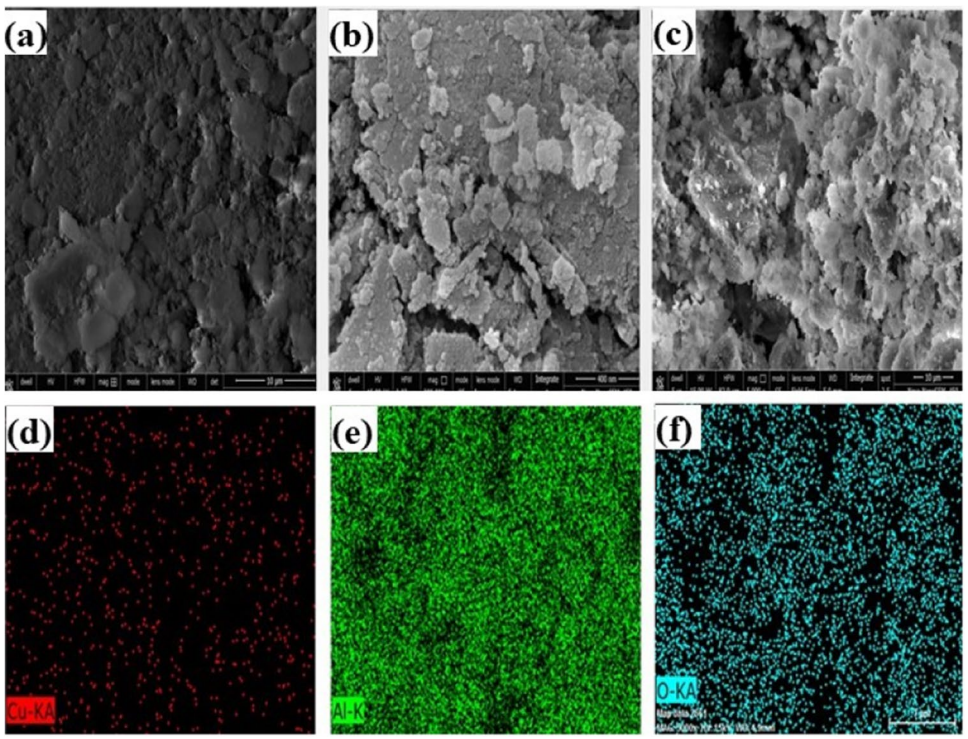

Fig. 2 SEM visuals of (**a**) AA, (**b**) pristine 1% Cu/AA, (**c**) spent 1% Cu/AA; EDX mapping of 1% Cu/AA dispersion of (**d**) copper, (**e**) alumina, (**f**) oxygen

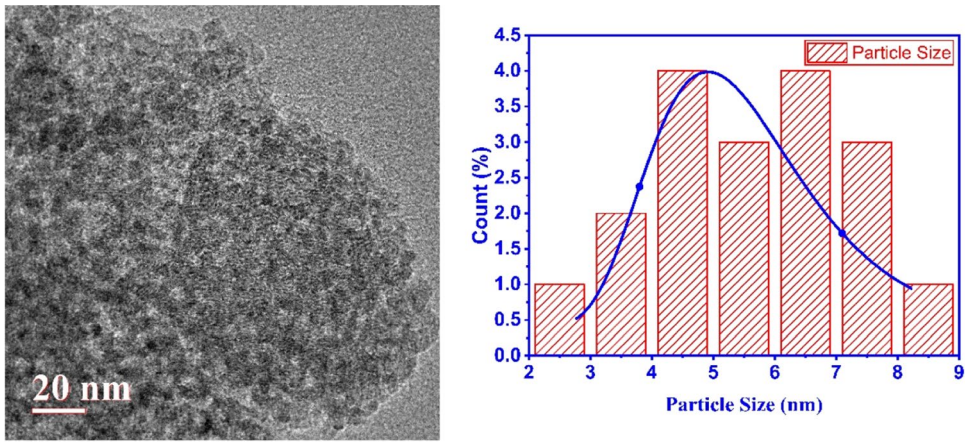

Fig. 3 TEM analysis of 1% Cu/AA

(a) TEM image of 1% Cu/AA **(b) Particle size distribution**

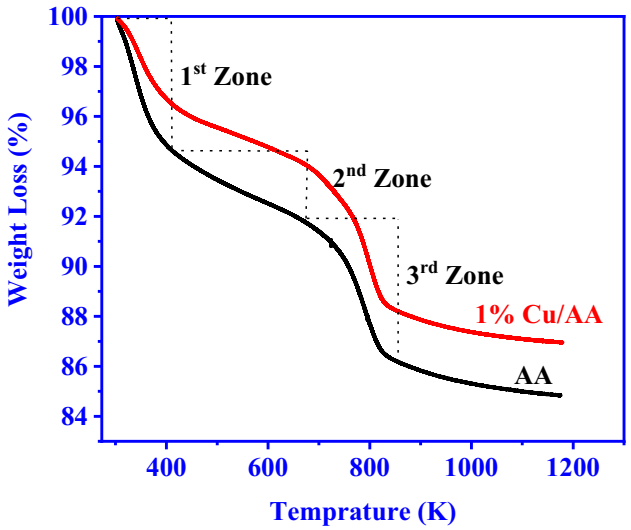

Fig. 4 TGA curves of AA and 1% Cu/AA

to AA, a film-like structure was observed, which may be attributed to multi-layer copper deposition on alumina beads. After CWPO treatment, the surface became rougher (Fig. 2(c)), and the pores gets widened due to catalytic adsorption and desorption of reactant and product molecules within the pore of 1% Cu/AA. Furthermore, as illustrated in Fig. 2 (c), rough surface was noticed, and the obtained results are in line with the existing literature (Suresh et al. 2012). The active metal dispersion on the support material has been confirmed by EDX mapping. It was found that copper (Fig. 2(d)), alumina (Fig. 2(e)), and oxygen species (Fig. 2(f)), are the major elements in a 1% Cu/AA catalyst. Furthermore, on the catalyst surface, copper has been uniformly distributed without forming any clusters.

Morphology of 1% Cu/AA catalyst was observed using TEM analysis. Active copper particle morphology is depicted in Fig. 3(a). It was observed that the active metal, copper, dispersed with a slight agglomeration on AA. Furthermore, the copper particle size distribution was calculated using a TEM image, and the average copper particle size was in the range of 2 to 9 nm. The average particle size was approximately 5 nm, shown in Fig. 3(b) (Mokrane et al. 2016), confirming the presence of Cu metal on the surface of AA (Li et al. 2001).

The stability of the synthesized catalysts was evaluated using TGA (Fig. 4) at temperatures ranging from 303 to 1173 K in an air atmosphere at a heating rate of 10 K/min using a sample weight of 15 mg. Both samples demonstrate significant weight loss in all three zones. The initial weight loss zone was noticed below 393 K due to the evaporation of water molecules in the pore of the AA framework; the weight loss effects of AA and 1% Cu/AA were found to be 4.9% and 2.9%, respectively. Furthermore, the presence of volatile substances within the AA pores was found to be the cause of the second weight loss zone, which was observed between 393 and 673 K. The weight loss in the second zone was 3.4% for AA and 2.8% for Cu/AA, respectively. The third zone of weight loss occurred between 673 and 833 K, which was credited to the thermal decomposition of AA, where 5.8 and 5.9% of weight loss were witnessed for AA and 1% Cu/AA, respectively. Therefore, a temperature of 673 K is suitable for the calcination process during the synthesis of the catalyst (Cu/AA). The percentage of total weight loss of 15% and 13% loss was observed AA and Cu/AA in the range of 303 to 1173 K (Wolanov et al. 2014).

Effect of operating parameters on degradation of catechol

Preliminary investigation

The preliminary experiments were conducted to determine the influence of various parameters on degradation rate of

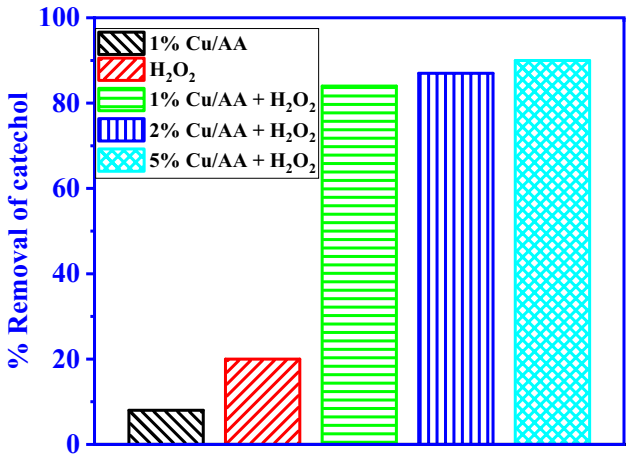

Fig. 5 Preliminary experiments for catechol removal

catechol shown in Fig. 5. In the absence of H_2O_2, the adsorption capacity of the synthesized catalyst 1% Cu/AA was determined. Consequently, approximately 8% removal was attained using a 1% Cu/AA catalyst at a pH of 7, a catalyst dose of 1 g/L, a reaction temperature of 323 K, and an initial concentration of catechol 100 mg/L. The oxidation capacity of pure H_2O_2 was investigated (as a control) in the absence of 1% Cu/AA, and 20% catechol removal was attained with a H_2O_2/catechol = 1.5. Additionally, the CWPO of catechol was investigated using H_2O_2 with the presence of catalyst (1% Cu/AA), and significant removal was achieved. The experimental results demonstrated that H_2O_2 or 1% Cu/AA alone did not result in significant degradation of catechol (e.g., < 20%), indicating the substantial degradation of catechol was achieved with a combination of catalyst and oxidant (i.e., via the CWPO process). Effect of active metal on AA for CWPO of catechol has been investigated using 1%, 2%, and 5% copper loaded AA (1% Cu/AA, 2% Cu/AA and 5% Cu/AA). As shown on Fig. 5, increase in active metal loading from 1% to 5%, the catechol removal was increased. However, the degradation was not appreciable quantity, this may be due to multilayer dispersion of active metal species on the AA surface; consequently, removal was not appreciable. Therefore, the further investigation 1% Cu/AA was used in CWPO process.

Effect of pH on degradation of catechol

Solution pH appears to have an influence on the physicochemical properties, surface charge of 1% Cu/AA, and catechol adsorption and desorption (Gosu et al. 2018a). In this study, the degradation of catechol was investigated by altering the initial pH of test solution in the range of 2–10 with a catalyst dose of 10 g/L, 100 mg/L initial concentration of catechol, a stoichiometric ratio H_2O_2/catechol of 1.5, reaction time of 4 h, and maintained 323 K thought out the study. As shown in Fig. 6 (a), catechol removal increased as the initial pH varied from 2 to 6, and 85% catechol removal was achieved at pH 6. The pKa value of catechol is 9.48 (Shakir et al. 2008), i.e., at pH ≤ 9.48, catechol is positively charged, while at pH ≥ 9.48, it is negatively charged. The PZC (point of zero charge) of the pristine 1% Cu/AA was noticed to be ~ 5 (Fig. 6(b)); thus, the 1% Cu/AA surface acts as electrically neutral when catechol solution has a pH of 5, a negative one if pH > 5, and a positive one if pH < 5 (Yadav and Srivastava 2017). Maximum removal of catechol was observed when the pH was between 5 and 6 (Fig. 6(a)), presumably due to the attraction of ionic forces between the catechol and Cu/AA (Al-Degs et al. 2008). Near the PZC, the maximum removal was achieved, which is in good agreement the literature (Gulicovski et al. 2008). At a higher pH (pH > 6), removal efficiency was declined continuously as at higher pH weak van der Waal forces are predominant between negative charged Cu/AA and uncharged catechol molecules, resulting in a decrease in the removal efficiency of catechol. Thus, pH 6 was revealed to be suitable and applied in subsequent studies.

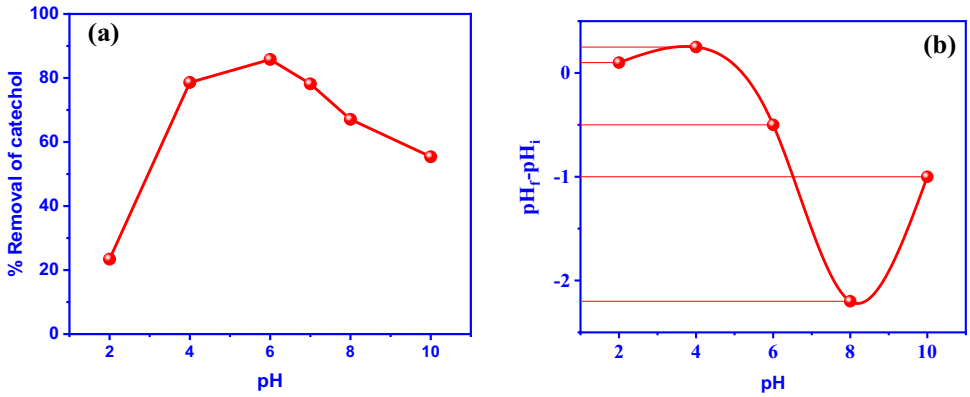

Fig. 6 The influence of pH on CWPO of catechol (dose of 1% Cu/AA = 10 g/L; reaction time = 4 h; T = 323 K; initial catechol concentration = 100 mg/L; H_2O_2/catechol = 1.5): (**a**) Effect of initial pH on catechol removal; and (**b**) Point of zero charge of 1% Cu/AA

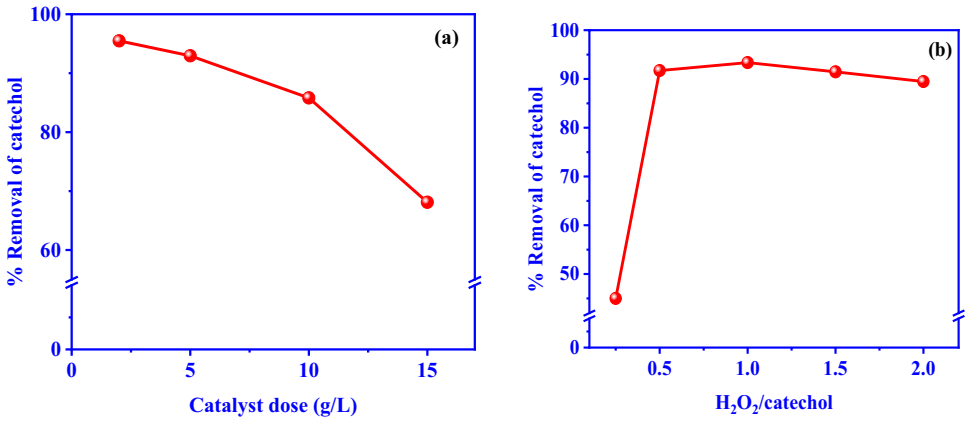

Fig. 7 **a** Influence of catalyst 1% Cu/AA dose on CWPO of catechol (pH = 6, time = 4 h T = 323 K, initial catechol concentration = 100 mg/L, H_2O_2/catechol = 1.5); **b** Effect of H_2O_2 dose on CWPO of catechol (pH = 6; catalyst dose of 1% Cu/AA = 2 g/L, time = 4 h; and T = 323 K)

Effect of catalyst dose on degradation of catechol

In the CWPO process, identifying the optimum amount of catalyst is an essential factor that reduces the overall treatment cost. Figure 7 (a) shows that with an increase in catalyst dose from 2 to 15 g/L, while keeping other parameters as constant. Experimental results observed that, with an increase in catalyst dose from 2 to 15 g/L, the degradation of catechol was declined from 95 to 65%. The observed trend was elucidated by self-scavenging effect of hydroxyl radical at surplus catalyst dose as shown in Eq. (3). The acquired results are consistent with the published literature (Yadav and Srivastava 2017). The author was not conducted below 2 g/L because, conducting experiments below 2 g/L is difficult (in 100 ml reaction mixture one single granule/ball of AA contributed 2 g/L). Thus, the optimal catalyst dose of 2 g/L was discovered to be effective and was employed in further tests.

$$Cu^{1+}/AA + HO^{\bullet} \rightarrow Cu^{2+}/AA + HO^{\bullet} \quad (3)$$

Effect of H_2O_2 concentration on degradation of catechol

Catechol's CWPO primarily depends on the generation of hydroxyl radicals, which is proportional to the amount of hydrogen peroxide used. To investigate the effect of the H_2O_2 dose, the stoichiometry ratio of H_2O_2/catechol was varied from 0.5 to 2 times while all other parameters remained constant. As shown in the Fig. 7 (b), catechol degradation increased as the stoichiometry ratio of H_2O_2/catechol increased to 0.5, beyond which the improvement was insignificant. The phenomenon could be because an excess of formed hydroxyl radicals ($^{\bullet}OH$) is converted to hydroperoxyl radicals ($HOO^{\bullet}$). The oxidation capacity of hydroperoxyl radicals ($HOO^{\bullet}$) was less than that of $^{\bullet}OH$, thereby not making more contribution to the oxidative degradation of the catechol (Priyanka et al. 2014). Furthermore, the degradation of catechol increased as the stoichiometric ratio increased up to a critical ratio. The degradation rate decreases due to the scavenging effect. As a result, undesirable intermediates can be avoided by using the optimal amount of H_2O_2. A similar pattern of picoline degradation was observed using the Cu/SBA-15 catalyst in the CWPO process (Subbaramaiah et al. 2013b). In the following studies, the optimal H_2O_2/catechol was set to 0.5.

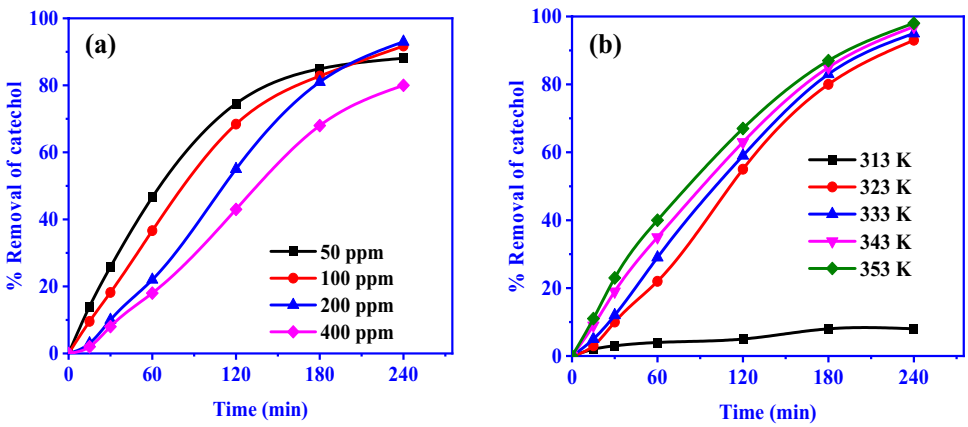

Fig. 8 **a** Effect of initial concentration of catechol on CWPO (pH = 6; catalyst dose of 1% Cu/AA = 2 g/L, time = 4 h, T = 323 K, H_2O_2/catechol = 0.5); (**b**) Effect of temperature on CWPO of catechol (pH = 6; catalyst dose of 1% Cu/AA = 2 g/L, time = 4 h, initial catechol concentration = 200 mg/L; and H_2O_2/catechol = 0.5)

Effect of initial concentration of catechol on degradation of catechol

Figure 8 (a) shows that the percentage removal of catechol was increased with an increase in time for all the initial concentrations of catechol. Besides, the degradation of catechol was decreased with an increase in the initial concentration of catechol due to availability of the sufficient amount of hydroxyl radical. Furthermore, for the fixed catalyst dose as the concentration of catechol increases the availability of number of active sites decreases, thereby the generation of hydroxyl radicals decreases resulting in a decrease in the percentage removal of catechol. The removal percentage of catechol for the initial catechol concentration of 50, 100, 200, and 400 ppm were 95.33%, 96%, 91.33%, and 71.72%, respectively in a 4-h duration. Thereafter 4 h, the insignificant removal was perceived (data not shown); as a result, the optimal initial catechol concentration of 200 ppm was chosen for further investigation.

Effect of temperature on degradation of catechol

The reaction temperature is a very significant factor which influence the CWPO process and controls the formation of •OH radical during the course of reaction. Figure 8 (b) shows that as the temperature increases, the % removal of catechol increases as increasing temperature would accelerate the reaction rate by increasing the formation of hydroxyl radicals and a decrease in their scavenging; furthermore, the generated hydroxyl radical reacts with catechol, degrading it non-selectively and converting it to non-toxic organic compounds. At 313 K, only 10% degradation efficiency was observed, while 90% removal was noticed at 323 K, beyond which an additional increase in temperature did not increase the removal efficiency significantly, which may be attributed to the self-scavenging of hydroxyl radical at a higher temperature. Therefore, 323 K was taken as optimum.

TOC measurements were used to describe catechol mineralization. At optimum conditions (catechol initial concentration = 200 mg/L; 1% Cu/AA dose = 2 g/L; temperature = 323 K; pH = 6; and H_2O_2/catechol = 0.5), the total TOC removal was 87%.

Reusability study

Recyclability is one of the important criteria to ensure stability and commercial applicability of the catalyst. The reusability test was conducted at optimized condition without using any regeneration technique. 1% Cu/AA catalyst has been reused up to five cycles and results are depicted in Fig. 9. It observed that around ~ 15% decline in removal efficiency from the first cycle to the fifth cycle. The catechol removal was declined from 93 to 79% for the 1st cycle to 5th cycle. The obtained results concluded that the synthesized catalyst exhibited stable catalytic activity with marginal decrease in catalytic activity (Gosu et al. 2018a; Sikarwar et al. 2023).

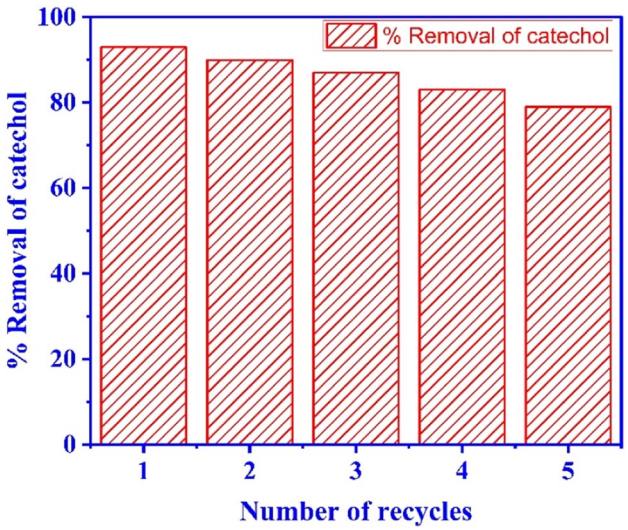

Fig. 9 Reusability study of 1% Cu/AA for mineralization of catechol

Kinetics

Kinetic studies were conducted at various temperatures while maintaining other reaction parameters constant, such as pH 6, catalyst dose 2 g/L, initial concentration of catechol 200 mg/L, and H_2O_2/catechol 0.5. The observed catechol degradation data were fitted using pseudo-first- (Eq. (4)) and pseudo-second-order kinetics (Eq. (5)) as follows:

$$ln\left(\frac{C_i}{C_f}\right) = k_1 t \tag{4}$$

$$\frac{1}{C_f} = \frac{1}{C_i} + k_2 t \tag{5}$$

where C_i denotes the catechol initial concentration; C_f implies the concentration of catechol at any time t; k_1 represents the rate constant for pseudo-first-order (1/min); and k_2 for pseudo-second-order (1/mg-min).

The values of the rate constants for the two models are compared and summarized in Table 2. Pseudo-first-order kinetics exhibited greater correlation values ($R^2 > 0.90$) with the experimental data when compared to second-order kinetics. In addition, the apparent rate constant increased with increasing temperature, which is evidenced that the catechol degradation process follows pseudo-first-order kinetics (Subbaramaiah et al. 2013a). The apparent activation energy (E) was estimated using the Arrhenius equation by plotting ln k vs 1/T. The activation energy

Table 2 Kinetic and thermodynamic properties of catechol oxidation

	Pseudo-first order			Pseudo-second order		
Temperature (K)	K_f (1/min)	R^2	E_a (kJ/mol)	k_s (1/mg.min)	R^2	E_a (kJ/mol)
313	0.0006	0.9761	67	0.000002	0.9202	120
323	0.0137	0.9004		0.0002	0.7662	
333	0.0154	0.9078		0.0003	0.7313	
343	0.0176	0.9027		0.0005	0.6651	

for catechol degradation by 1% Cu/AA was estimated to be 67 kJ/mole and 120 kJ/mole for pseudo-first-order and pseudo-second-order reaction respectively. Inchaurrondo et al. (2012) examined the kinetics of phenol degradation in the presence of a CuO/Al_2O_3 catalyst using hydrogen peroxide, and the activation energy was determined to be 56.8 kJ/mol (Inchaurrondo et al. 2012). The obtained results are consistent with the current literature.

Reaction mechanism for catechol

The 1% Cu/AA catalyst was used for catechol degradation at optimum conditions (initial concentration of catechol = 200 mg/L; pH = 6; H_2O_2/catechol stoichiometry ratio = 0.5; catalyst dose of 1% Cu/AA = 2 g/L; and T = 323 K), and mass spectroscopy (UPLC-MS) was used to investigate the mechanism of the catechol CWPO reaction. Figure 10 shows catechol before reaction and after degradation using LC–MS. Accordingly, Fig. 11 depicts the proposed mechanism for catechol degradation into various intermediates during the course of the reaction. Hydrogen peroxide was used as an oxidizing agent, which generates HO· radicals in the presence of catalyst Cu(II)/Cu(I) (Eq. 4–6).

$$Cu^{2+} + H_2O_2 \rightarrow Cu^{1+} + H^+ + HOO^{\bullet} \quad (6)$$

$$Cu^{1+} + H_2O_2 \rightarrow Cu^{2+} + OH^- + HO^{\bullet} \quad (7)$$

$$Cu^{2+} + HOO^{\bullet} \rightarrow Cu^{1+} + H^+ + O_2 \quad (8)$$

The catechol molecules in the solution react with generated HO· radicals and convert into intermediate compounds (Eq. (7)) such as pyrogallol, 2-hydroxy-O-quinone, benzaldehyde, 1-cyclohexane 1-ol. Furthermore, these compounds were further reacted with hydroxyl radicals, producing simple organic acids such as cis-cis muconic acid, maleinaldehydic acid, maleic acid, and glutaconic acid. Henceforth, these organic acids transform into light acids and aldehydes (acetaldehyde, crotonic acid, formic acid, oxalic acid, glyoxal, and 3-oxopropanoic acid) in the presence of hydroxyl radicals (M'hemdi et al. 2012). As a result, these intermediate products are finally mineralized into simple, harmless compounds (CO_2 and water).

$$\text{Catechol} \xrightarrow{HOO^{\bullet}/HO^{\bullet}} \text{Intermediate organic compounds} \xrightarrow{HOO^{\bullet}/HO^{\bullet}} CO_2 + H_2O_2 \quad (9)$$

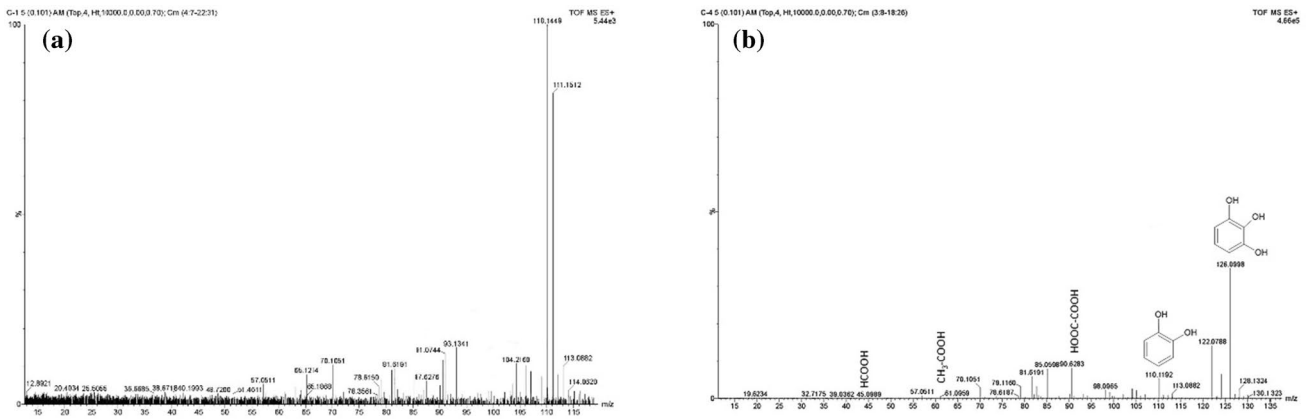

Fig. 10 LC–MS evidence of CWPO of catechol under the optimal conditions (initial concentration of catechol = 200 mg/L; pH = 6; H_2O_2/catechol stoichiometry ratio = 0.5; catalyst dose of 1% Cu/AA = 2 g/L; and T = 323 K) (**a**) Before CWPO reaction; (**b**) After CWPO reaction

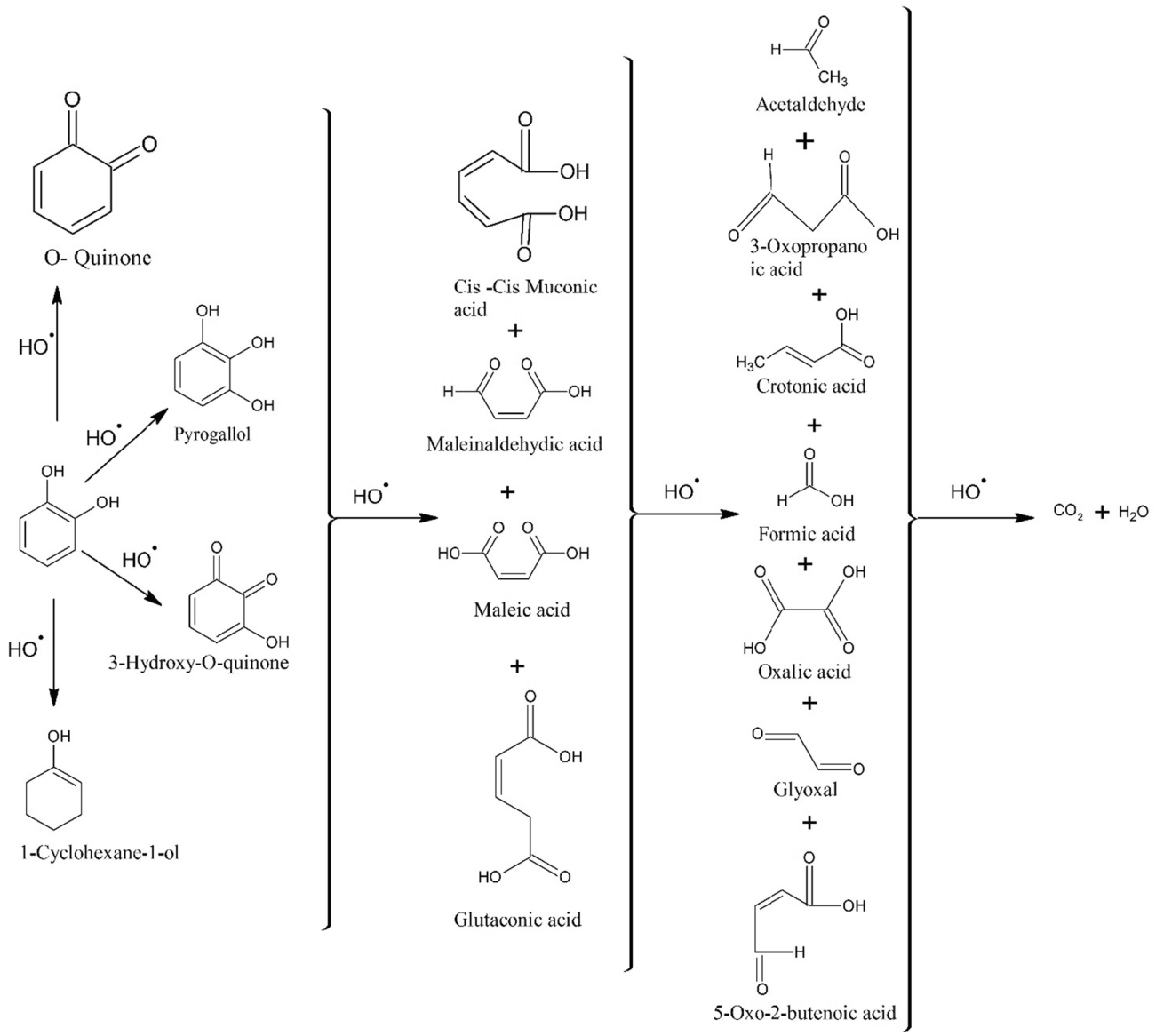

Fig. 11 Proposed reaction mechanism for catechol oxidation

Conclusion

Catechol mineralization was investigated by employing 1% Cu/AA in CWPO process. From the characterization study, it was confirmed that 1% Cu was successfully incorporated into the AA framework with the copper particle size of 2–9 nm. Furthermore, catechol degradation using 1% Cu/AA was optimized at conditions of initial catechol concentration = 200 mg/L; catalyst dose = 2 g/L; temperature = 323 K; pH = 6; and H_2O_2/catechol stoichiometric ratio = 0.5. The percentage removal of catechol and TOC at the optimum conditions were 94% and 87%, respectively. The MS analysis provided the information of generated organic compounds during the CWPO of catechol. The degradation of catechol follows the pseudo-first-order kinetics. The synthesized catalyst showed a stable performance up to five cycles. Therefore, this study showed that 1% Cu/AA effective for the degradation of the catechol.

Author contribution All authors contributed to make final draft. Dr. Vijayalakshmi Gosu: Validation and Writing—Review & Editing. Archana Dhakar: Investigation, and Writing—Original Draft. Prof. Tian C. Zhang and Prof. Rao Y. Surampalli: Reviewed critically for important intellectual content. All authors read and approved the final manuscript. Dr. Verraboina Subbaramaiah: Conceptualization, Supervision, Project administration.

Funding The authors are thankful to Malaviya National Institute of Technology Jaipur for the support to carry out the work.

Data availability All data generated are analyzed during this study and are included in this present article.

Declarations

Ethics approval This article does not contain any studies with human participants or animals performed by any of the authors. The manuscript is not submitted to more than one journal for simultaneous consideration.

Consent to participate Informed consent was obtained from all individual participants included in the study.

Consent for publication All individual participants consent to publish this article.

Competing interests The authors declare no competing interests.

References

Aghapour AA, Moussavi G, Yaghmaeian K (2015) Degradation and COD removal of catechol in wastewater using the catalytic ozonation process combined with the cyclic rotating-bed biological reactor. J Environ Manage 157:262–266. https://doi.org/10.1016/j.jenvman.2015.02.036

Ahmed N, Siddiqui ZN (2014) Mesoporous alumina sulphuric acid: a novel and efficient catalyst for on-water synthesis of functionalized 1,4-dihydropyridine derivatives via β-enaminones. J Mol Catal A Chem 394:232–243. https://doi.org/10.1016/j.molcata.2014.07.015

Al-Degs YS, El-Barghouthi MI, El-Sheikh AH, Walker GM (2008) Effect of solution pH, ionic strength, and temperature on adsorption behavior of reactive dyes on activated carbon. Dye Pigment 77:16–23. https://doi.org/10.1016/j.dyepig.2007.03.001

Bian Z, Zhong W, Yu Y et al (2021) Dry reforming of methane on Ni/mesoporous-Al2O3 catalysts: effect of calcination temperature. Int J Hydrogen Energy 46:31041–31053. https://doi.org/10.1016/j.ijhydene.2020.12.064

Cordi EM, O'Neill PJ, Falconer JL (1997) Transient oxidation of volatile organic compounds on a CuO/AL2O3 catalyst. Appl Catal B Environ 14:23–36. https://doi.org/10.1016/S0926-3373(97)00009-X

di Luca C, Massa P, Grau JM et al (2018) Highly dispersed Fe3+-Al2O3 for the Fenton-like oxidation of phenol in a continuous up-flow fixed bed reactor. Enhancing catalyst stability through operating conditions. Appl Catal B Environ 237:1110–1123. https://doi.org/10.1016/j.apcatb.2018.05.032

Elboughdiri N, Mahjoubi A, Shawabkeh A et al (2015) Optimization of the degradation of hydroquinone, resorcinol and catechol using response surface methodology. Adv Chem Eng Sci 05:111–120. https://doi.org/10.4236/aces.2015.52012

Fasanya OO, Al-Hajri R, Ahmed OU et al (2019) Copper zinc oxide nanocatalysts grown on cordierite substrate for hydrogen production using methanol steam reforming. Int J Hydrogen Energy 44:22936–22946. https://doi.org/10.1016/j.ijhydene.2019.06.185

García-Mora AM, Portilla-Delgado CS, Torres-Palma RA et al (2021) Catalytic wet peroxide oxidation to remove natural organic matter from real surface waters at urban and rural drinking water treatment plants. J Water Process Eng 42:102136. https://doi.org/10.1016/J.JWPE.2021.102136

Gogoi A, Navgire M, Sarma KC, Gogoi P (2017) Fe3O4-CeO2metal oxide nanocomposite as a Fenton-like heterogeneous catalyst for degradation of catechol. Chem Eng J 311:153–162. https://doi.org/10.1016/j.cej.2016.11.086

Gosu V, Arora S, Subbaramaiah V (2020) Simultaneous degradation of nitrogenous heterocyclic compounds by catalytic wet-peroxidation process using box-behnken design. Environ Eng Res 25:488–497. https://doi.org/10.4491/eer.2019.159

Gosu V, Dhakar A, Sikarwar P, et al (2018a) Wet peroxidation of resorcinol catalyzed by copper impregnated granular activated carbon. J Environ Manage 223. https://doi.org/10.1016/j.jenvman.2018.06.093

Gosu V, Dhakar A, Sikarwar P et al (2018b) Wet peroxidation of resorcinol catalyzed by copper impregnated granular activated carbon. J Environ Manage 223:825–833. https://doi.org/10.1016/J.JENVMAN.2018.06.093

Gosu V, Sikarwar P, Subbaramaiah V (2018c) Mineralization of pyridine by CWPO process using nFe^0/GAC catalyst. J Environ Chem Eng 6. https://doi.org/10.1016/j.jece.2018.01.017

Gulicovski JJ, Čerović LS, Milonjić SK (2008) Point of zero charge and isoelectric point of alumina. Mater Manuf Process 23:615–619. https://doi.org/10.1080/10426910802160668

Hachemaoui M, Molina CB, Belver C et al (2021) Metal-loaded mesoporous mcm-41 for the catalytic wet peroxide oxidation (Cwpo) of acetaminophen. Catalysts 11:1–17. https://doi.org/10.3390/catal11020219

Hu X, Lei L, Chu HP, Yue PL (1999) Copper/activated carbon as catalyst for organic wastewater treatment. Carbon N Y 37:631–637. https://doi.org/10.1016/S0008-6223(98)00235-8

Inchaurrondo NS, Massa P, Fenoglio R et al (2012) Efficient catalytic wet peroxide oxidation of phenol at moderate temperature using a high-load supported copper catalyst. Chem Eng J 198–199:426–434. https://doi.org/10.1016/j.cej.2012.05.103

Kermani M, Kakavandi B, Farzadkia M et al (2018) Catalytic ozonation of high concentrations of catechol over TiO2@Fe3O4 magnetic core-shell nanocatalyst: optimization, toxicity and degradation pathway studies. J Clean Prod 192:597–607. https://doi.org/10.1016/j.jclepro.2018.04.274

Kim MJ, Lee MW, Lee KY (2021) Improved catalytic wet peroxide oxidation of phenol over Pt-Fe2O3/SBA-15: influence of platinum species and DFT calculations. Appl Surf Sci 541:148409. https://doi.org/10.1016/j.apsusc.2020.148409

Kıpçak İ, Kurtaran Ersal E (2021) Catalytic wet peroxide oxidation of a real textile azo dye Cibacron Red P-4B over Al/Fe pillared bentonite catalysts: kinetic and thermodynamic studies. React Kinet Mech Catal 132:1003–1023. https://doi.org/10.1007/s11144-021-01962-5

Kumar A, Kumar S, Kumar S (2003) Adsorption of resorcinol and catechol on granular activated carbon: equilibrium and kinetics. Carbon N Y 41:3015–3025. https://doi.org/10.1016/S0008-6223(03)00431-7

Li YH, Wang S, Cao A et al (2001) Adsorption of fluoride from water by amorphous alumina supported on carbon nanotubes. Chem Phys Lett 350:412–416. https://doi.org/10.1016/S0009-2614(01)01351-3

Lofrano G, Rizzo L, Grassi M, Belgiorno V (2009) Advanced oxidation of catechol: a comparison among photocatalysis, Fenton and photo-Fenton processes. Desalination 249:878–883. https://doi.org/10.1016/j.desal.2009.02.068

M'hemdi A, Dbira B, Abdelhedi R et al (2012) Mineralization of catechol by Fenton and photo-Fenton processes. Clean - Soil Air Water 40:878–885. https://doi.org/10.1002/clen.201100376

Mandal A, Ojha K, De AK, Bhattacharjee S (2004) Removal of catechol from aqueous solution by advanced photo-oxidation process. Chem Eng J 102:203–208. https://doi.org/10.1016/j.cej.2004.05.007

Márquez JJR, Levchuk I, Sillanpää M (2018) Application of catalytic wet peroxide oxidation for industrial and urban wastewater treatment: a review. Catalysts 8:673. https://doi.org/10.3390/catal8120673

Mishra S, Bal R, Dey RK (2021) Heterogeneous recyclable copper oxide supported on activated red mud as an efficient and stable catalyst for the one pot hydroxylation of benzene to phenol. Mol Catal 499. https://doi.org/10.1016/j.mcat.2020.111310

Mokrane T, Boudjahem AG, Bettahar M (2016) Benzene hydrogenation over alumina-supported nickel nanoparticles prepared by polyol method. RSC Adv 6:59858–59864. https://doi.org/10.1039/c6ra08527j

Moussavi G, Aghapour AA, Yaghmaeian K (2014) The degradation and mineralization of catechol using ozonation catalyzed with MgO/GAC composite in a fluidized bed reactor. Chem Eng J 249:302–310. https://doi.org/10.1016/j.cej.2014.03.059

Mukherjee S, Kumar S, Misra AK, Fan M (2007) Removal of phenols from water environment by activated carbon, bagasse ash and wood charcoal. Chem Eng J 129:133–142. https://doi.org/10.1016/j.cej.2006.10.030

Priyanka SV, Srivastava VC, Mall ID (2014) Catalytic oxidation of nitrobenzene by copper loaded activated carbon. Sep Purif Technol 125:284–290. https://doi.org/10.1016/J.SEPPUR.2014.01.045

Qin L, Yu X, Wang K, Wang X (2022) Spherical ZVI/Mn-C bimetallic catalysts for efficient Fenton-like reaction under mild conditions. Catalysts 12. https://doi.org/10.3390/catal12040444

Sánchez-De La Torre F, Rivera De La Rosa J, Kharisov BI, Lucio-Ortiz CJ (2013) Preparation and characterization of cu and ni on alumina supports and their use in the synthesis of low-temperature metal-phthalocyanine using a parallel-plate reactor. Materials (basel) 6:4324–4344. https://doi.org/10.3390/ma6104324

Shakir K, Ghoneimy HF, Elkafrawy AF et al (2008) Removal of catechol from aqueous solutions by adsorption onto organophilic-bentonite. J Hazard Mater 150:765–773. https://doi.org/10.1016/j.jhazmat.2007.05.037

Sikarwar P, Nemiwal M, Gosu V, Subbaramaiah V (2023) Adsorptive denitrogenation of indole from model fuel oil over Co-MAC: adsorption mechanisms and competitive adsorption. J Indian Chem Soc 100:100801. https://doi.org/10.1016/j.jics.2022.100801

Srivastav A, Srivastava VC (2009) Adsorptive desulfurization by activated alumina. J Hazard Mater 170:1133–1140. https://doi.org/10.1016/j.jhazmat.2009.05.088

Subbaramaiah V, Srivastava VC, Mall ID (2013a) Optimization of reaction parameters and kinetic modeling of catalytic wet peroxidation of picoline by Cu/SBA-15. Ind Eng Chem Res 52. https://doi.org/10.1021/ie400124d

Subbaramaiah V, Srivastava VC, Mall ID (2013b) Catalytic activity of Cu/SBA-15 for peroxidation of pyridine bearing wastewater at atmospheric condition. AIChE J 59. https://doi.org/10.1002/aic.14017

Subramanyam R, Mishra IM (2007) Biodegradation of catechol (2-hydroxy phenol) bearing wastewater in an UASB reactor. Chemosphere 69:816–824. https://doi.org/10.1016/j.chemosphere.2007.04.064

Suresh S, Vijayalakshmi G, Rajmohan B, Subbaramaiah V (2012) Adsorption of benzene vapor onto activated biomass from cashew nut shell: batch and column study. Recent Patents Chem Eng 5:116–133. https://doi.org/10.2174/2211334711205020116

Thakur C, Srivastava VC, Mall ID, Hiwarkar AD (2017) Modelling of binary isotherm behaviour for the adsorption of catechol with phenol and resorcinol onto rice husk ash. Indian Chem Eng 59:312–334. https://doi.org/10.1080/00194506.2017.1281770

Wolanov Y, Shurki A, Prikhodchenko PV et al (2014) Aqueous stability of alumina and silica perhydrate hydrogels: experiments and computations. Dalt Trans 43:16614–16625. https://doi.org/10.1039/c4dt01024h

Yadav B, Srivastava VC (2017) Catalytic peroxidation of recalcitrant quinoline by ceria impregnated granular activated carbon. Clean Technol Environ Policy 19:1547–1555. https://doi.org/10.1007/s10098-016-1315-8

Yang X, He J, Sun Z et al (2016) Effect of phosphate on heterogeneous Fenton oxidation of catechol by nano-Fe3O4: Inhibitor or stabilizer? J Environ Sci (china) 39:69–76. https://doi.org/10.1016/j.jes.2015.11.007

Zawadzki M, Staszak W, López-Suárez FE et al (2009) Preparation, characterisation and catalytic performance for soot oxidation of copper-containing ZnAl2O4 spinels. Appl Catal A Gen 371:92–98. https://doi.org/10.1016/j.apcata.2009.09.035